Effect of the ionic liquid 1-ethyl-3-methylimidazolium acetate on the phase transition of starch: dissolution or gelatinization?

Sainimili Mateyawa [a], David Fengwei Xie [a,*], Rowan W. Truss [b], Peter J. Halley [a,b], Timothy M. Nicholson [b], Julia L. Shamshina [c], Robin D. Rogers [c], Michael W. Boehm [b], Tony McNally [d]

[a] *Australian Institute for Bioengineering and Nanotechnology, The University of Queensland, Brisbane, Qld 4072, Australia*

[b] *School of Chemical Engineering, The University of Queensland, Brisbane, Qld 4072, Australia*

[c] *Center for Green Manufacturing and Department of Chemistry, The University of Alabama, Tuscaloosa, AL 35487, USA*

[d] *School of Mechanical and Aerospace Engineering, Queen's University Belfast, BT9 5AH, UK*

Abbreviations: waxy maize starch, WMS; regular maize starch, RMS; Gelose 50, G50; Gelose 80, G80; 1-ethyl-3-methylimidazolium acetate, [EMIM][OAc]; T_o, onset temperature; T_p, peak temperature; T_c, conclusion temperature; ΔT, temperature range, i.e. T_c–T_o; ΔH, enthalpy.

[*] Corresponding author. Tel.: +61 7 3346 3199; fax: +61 7 3346 3973.

Email address: f.xie@uq.edu.au; fwhsieh@gmail.com (D. F. Xie)

ABSTRACT

This work revealed that the interactions between starch, the ionic liquid 1-ethyl-3-methylimidazolium acetate ([Emim][OAc]), and water might contribute to the phase transition (gelatinization, dissolution, or both) of native starch at reduced temperature. Using mixtures of water and [Emim][OAc] at certain ratios (7.2/1 and 10.8/1, mol/mol), both the gelatinization and dissolution of the starch occur competitively, but also in a synergistic manner. At lower [Emim][OAc] concentration (water/[Emim][OAc] molar ratio ≥ 25.0/1), mainly gelatinization occurs which is slightly impeded by the strong interaction between water and [Emim][OAc]; while at higher [Emim][OAc] concentration (water/[Emim][OAc] molar ratio ≤ 2.8/1), the dissolution of starch is the major form of phase transition, possibly restricted by the difficulty of [Emim][OAc] to interact with starch.

[Graphical Abstract included]

Keywords:

Starch; Biopolymer dissolution; Ionic liquid; 1-ethyl-3-methylimidazolium acetate; Gelatinization; Phase transition

1. Introduction

Starch is a natural polymer with particular properties unlike those of traditional polymers. As a heterogeneous material, it has macromolecular structures bound in a granular superstructure; it normally has both linear (amylose) and branched (amylopectin) molecules; and it contains both amorphous and crystalline regions within its granules (Pérez, & Bertoft, 2010). When native starch granules are heated in water, their semicrystalline nature and three-dimensional architecture are gradually disrupted, resulting in a phase transition from the ordered granular structure into a disordered state in water, which is known as "gelatinization"(Atwell, Hood, Lineback, Varrianomarston, & Zobel, 1988; Lelievre, 1974; Ratnayake, Jackson, & Steve, 2008). Gelatinization is an irreversible process that includes several, often sequential steps, such as granular swelling, native crystalline melting (loss of birefringence), and molecular solubilization (Russo et al., 2009). The gelatinization process is essential in the processing of foods and emerging biodegradable starch-based materials.

For improving starch's processibility and product properties, adding new functionalities, and expanding the current applications, it is not uncommon to carry out processing of starch in environments containing substances other than water. Various plasticizers and additives for starch processing that have been used include polyols (glycerol, glycol, sorbitol, etc.) and nitrogen-containing compounds (urea, ammonium derived, and amines) (Liu, Xie, Yu, Chen, & Li, 2009; Xie, Halley, & Avérous, 2012). However, these plasticizers or additives either are not stable under normal processing conditions, can be lost from the final product, or are hydroscopic. An alternative class of materials known as ionic liquids (ILs), now commonly defined as salts which melt below 100 °C, has recently attracted much interest for the processing of biopolymers including starch. Many ILs, especially ones based on the imidazolium cation, outperform other

plasticizers and additives as they directly dissolve polysaccharides such as starch and thus can be used as an excellent media for polysaccharide plasticization and modification (Biswas, Shogren, Stevenson, Willett, & Bhowmik, 2006; El Seoud, Koschella, Fidale, Dorn, & Heinze, 2007; Wilpiszewska, & Spychaj, 2011; Zakrzewska, Bogel-Łukasik, & Bogel-Łukasik, 2010; Zhu et al., 2006). Furthermore, studies have shown that starch-based ionically conducting polymers or solid polymer electrolytes could be developed by using ILs as plasticizers, such as 1-allyl-3-methylimidazlium chloride ([Amim][Cl]), 1-butyl-3-methylimidazolium hexafluorophosphate ([Bmim][PF_6]), or 1-butyl-3-methylimidazolium trifluoromethanesulfonate ([Bmim][CF_3SO_3]) (Liew, Ramesh, Ramesh, & Arof, 2012; Ramesh, Liew, & Arof, 2011; Ramesh, Shanti, Morris, & Durairaj, 2011; Ramesh, Shanti, & Morris, 2012; Wang, Zhang, Liu, & He, 2009; Wang, Zhang, Wang, & Liu, 2009; Wang, Zhang, Liu, & Han, 2010b). Sankri et al. (2010) and Leroy, Jacquet, Coativy, Reguerre, & Lourdin (2012) have already done pioneering work using 1-butyl-3-methylimidazolium chloride ([Bmim][Cl]) as a new plasticizer in melt processing of starch-based materials and improvements in plasticization, electrical conductivity, and hydrophobicity were demonstrated.

It is worth noting that many of the ILs used previously to plasticize starch contained the corrosive [Cl^-] anion (e.g. [BMIM][Cl]) (Wilpiszewska, & Spychaj, 2011). By heat dispersion in this type of IL, macromolecular degradation of starch could be observed (Kärkkäinen, Lappalainen, Joensuu, & Lajunen, 2011; Stevenson, Biswas, Jane, & Inglett, 2007), due to acidic hydrolysis of glycosidic bonds in starch-based materials. Specifically, the reason for this degradation is the formation of HCl (as a result of the protonation of [Cl^-] anion in the presence of moisture), which can catalyze the depolymerization of starch (Kärkkäinen et al., 2011). Considering these issues, it has been suggested that ILs with non-halogen-containing anions such

as 1-ethyl-3-methylimidazolium acetate ([Emim][OAc]) (see Figure 1 for chemical structure) may be more suitable for the development of high-performance functional starch-based materials. [Emim][OAc] has a very low vapor pressure, high thermal stability, and relatively low viscosity at room temperature (Liu, & Budtova, 2012), which enables it to be used with starch in a wide range of processing conditions.

[Insert Figure 1 here]

Very recently, Liu, & Budtova (2012) carried out a quality study of gelatinization/dissolution of waxy maize starch in water–[Emim][OAc] mixtures of different ratios by microscopy. Compared with pure water or neat [Emim][OAc], the water–[Emim][OAc] mixtures of certain ratios produced better gelatinization and dissolution of starch at elevated temperature (Liu, & Budtova, 2012). Their results also showed that the dependence of gelatinization/dissolution parameters on the ratio of water/[EMIM][OAc] was quite complex. However, the mechanism of such gelatinization/dissolution was not well understood and it is unlikely that starch–IL gelatinization is best revealed using solely microscopy.

This paper focuses on understanding the role of water/[Emim][OAc] mixtures in starch gelatinization/dissolution and the establishment of the corresponding mechanisms. Maize starches with different amylose contents have been used. They are interesting because that they can be directly provided by nature and the varied amylose content has an impact on the native granular structures, processing behaviors, and final product properties (Chaudhary, Miler, Torley, Sopade, & Halley, 2008; Chaudhary, Torley, Halley, McCaffery, & Chaudhary, 2009; Li

et al., 2011; Tan, Flanagan, Halley, Whittaker, & Gidley, 2007; Wang et al., 2010a; Xie et al., 2009; Xie et al., 2012).

The three most recognized techniques for starch gelatinization characterization were used; namely differential scanning calorimetry (DSC), rapid visco analysis (RVA), and microscopy. DSC provides the possibility of analyzing the transition temperatures as well as the transition enthalpies, which correspond to the melting of crystalline structures in starch during heating. RVA, which is used as an industrial standard, detects the viscosity change of starch slurries during a pre-set controlled heating and cooling, where the gelatinization process (which results in viscosity changes) can be revealed. Microscopy is a simple but reliable method in the study of starch as it reveals the morphology (under normal light) and crystalline structures (under polarized light) of starch. To the best of our knowledge, this is the first work involving the use of these different techniques in the study of starch phase transitions in ionic liquid–water environments and the exploration of the possibility to dissolve starch at reduced temperature. Basic knowledge related to the use of ILs in starch processing is thus provided, which is valuable for future work.

2. Materials and Methods

2.1. Materials

Four varieties of commercially available maize starches were used in this work, including waxy maize starch (Mazaca 3401X) (WMS), regular maize starch (Avon Maize Starch) (RMS), Gelose 50 (G50), and Gelose 80 (G80). RMS was supplied by New Zealand Starch Ltd. (Onehunga, Auckland, New Zealand) and the other three starches were supplied by National Starch Pty Ltd. (Lane Cove NSW 2066, Australia). All starches were chemically unmodified

and the amylose contents for these four types of starches were 3.4%, 24.4%, 56.3% and 82.9%, respectively, as measured by Tan et al. (2007) using the iodine colorimetric method. The original moisture contents of the four starches were 12.4%, 14.1%, 13.6%, and 14.4%, respectively. Deionized water was used in all instances. [Emim][OAc] of purity ≥90%, produced by BASF, was supplied by Sigma-Aldrich. [Emim][OAc] was used as received without further purification but the purity was considered for molar ratio calculation. As [Emim][OAc] was in liquid form at room temperature, different ratios of water–[Emim][OAc] mixture could be easily prepared in vials for subsequent studies. Water and [Emim][OAc] were completely miscible according to the [Emim][OAc] specifications provided by BASF. The mass ratios of water/[Emim][OAc] used were 10/0, 9/1, 7/3, 5/5, 4/6, 2/8, and 0/10; and the related molar ratios were 1/0 (pure water), 96.0/1, 25.0/1, 10.8/1, 7.2/1, 2.8/1, 0.1/1 (also in Appendix A). Molar ratio will be used in the Results and Discussion sections, below.

2.2. DSC

A TA Q2000 DSC (TA Instruments, Inc., New Castle, DE 19720, USA) was used to investigate the thermal transition of native starches in water–[Emim][OAc] mixtures. 1.5–3 mg of starch was weighed into the 40 μL Tzero aluminium pan (TA Instruments), to which was then added, by a microsyringe, the water–[Emim][OAc] mixture, in the amount 10 times that of the starch. Then, a pin was used to gently mix starch with the plasticizer. After sealing, the pan was gently shaken for a few seconds. The mixing and shaking were to ensure the starch granules were completely immersed and equally dispersed in the liquid but did not sediment at the bottom of the pan. The pans thus prepared were transferred into the DSC machine for immediate analysis to avoid sedimentation of starch granules or time effects of the water–[Emim][OAc]

mixture on starch. An empty pan was used as a reference. The pans were heated from 20 °C to 120 °C at a scanning rate of 5 °C/min. The instrument was calibrated using indium as a standard. At least two runs were carried out for each sample to ensure the consistency of the results. The Universal Analysis 2000 (TA Instruments–Waters LLC) software was used to analyze the main gelatinization endotherm of the DSC traces for the onset (T_o), peak (T_p), and conclusion (T_c) temperatures, the thermal transition temperature range (ΔT, i.e. $T_c - T_o$), and the enthalpy (ΔH).

2.3. RVA

The pasting properties of all starch samples were determined with a rapid visco analyzer RVA 4 controlled by Thermocline for Windows version 2.2 (Newport Scientific Pty Ltd., Warriewood NSW 2102, Australia). The RVA sample preparation procedure and heating profile followed a previous study (Torley, Rutgers, D'Arcy, & Bhandari, 2004). Briefly, a 3.0 g starch sample was weighed into a sample test canister and 25.0 g of the water–[Emim][OAc] mixture was added. The RVA impeller was jogged up and down and rotated in the canister to suspend the starch in the liquid. The RVA canister and impeller were then positioned in the RVA and the trial started. The test profile involved stirring at 960 rpm for 10 s at 50 °C, stirring at 160 rpm for 50 s at 50 °C (this rotation rate was maintained in all subsequent stages of the test), heating from 50 °C to 95 °C within 225 s, holding at 95 °C for 300 s, cooling from 95 °C to 50 °C within 285 s, and holding at 50 °C for 300 s. The total test time was 1170 s (19.5 min).

The RVA pasting curve was analyzed to determine a series of characteristic parameters, including pasting temperature (temperature at which viscosity starts to increase), peak viscosity (maximum viscosity during heating to or holding at 95 °C), trough viscosity or holding strength (minimum viscosity after peak viscosity has been reached), and final viscosity (viscosity at the

end of run). Breakdown (difference between trough viscosity and peak viscosity) and setback (difference between final viscosity and trough viscosity) were calculated. However, this kind of analysis was not possible for some of the curves due to the irregularity of shape. The viscosity in RVA is expressed in rapid visco units (RVU)

2.4. Microscopy

A polarization microscope equipped with a CMOS camera was used in the experimental work. The magnification used was ×400 (40×10). Both normal and polarized light were used to obtain the microscopic images of the starch samples (native starches, and the starch samples from DSC and RVA) at room temperature. At least three replicates were performed for each sample to ensure consistent results.

For the observation of native starches, suspensions with 0.5% starch were prepared in glass vials. A small drop of starch suspension was transferred by a microsyringe onto a glass slide which was then covered by another glass slide. Silicon adhesive was used to seal the starch suspension between the two glass slides to avoid evaporation during observation.

Microscopic observation of starch samples after DSC treatment was also carried out. After DSC scanning to specific temperatures, the starch samples were rapidly cooled to room temperature. Immediately after that, the starch sample was taken out of the DSC pan for microscopic observation using the same method as for native starches. The sample was further dispersed if the particles were too dense.

189 *2.5. pH*

190 All pH values are shown for samples at room temperature. For measuring the pH value of
191 water–[EMIM]OAc mixture with starch, waxy maize starch was used as an example. In this
192 case, pH measurements were carried out according to the method ISI 26-5e of International
193 Starch Institute.

194

195 *2.6. Rheology*

196 Rheological measurements were carried out at 22 °C on a TA AR G2 stress controlled
197 rheometer using a 40 mm Titanium parallel-plate at a commanded gap of 30 μm; temperature
198 was controlled at the bottom plate using the peltier unit. To limit evaporation, 10 cSt silicone oil
199 (E200, Esco) was washed over the outer edge of the plate and a cover used over the geometry.

200 By using a narrow gap, we reduce the required sample volume and achieve shear rate of
201 10^5 s^{-1}. The narrow gap technique is detailed elsewhere (Davies, & Stokes, 2005, 2008). Briefly,
202 the gap error that arises from plate misalignment and other factors must be measured and then
203 several calculations were performed post-testing: (1) the gap error correction is applied to η; (2)
204 the parallel plate correction is applied to η, which accounts for the radial dependence of the shear
205 rate when using the parallel-plate; and (3) a check that the Reynolds number ($\mathrm{Re} = \rho h^2 \dot{\gamma}_R / \eta$) is
206 below 100, which is a test for secondary flow effects.

207

3. Results

3.1. Effect of water/[Emim][OAc] ratio on the gelatinization/dissolution of maize starches with different amylose contents.

Figure 2a–d show the DSC results of maize starches with different amylose content in water–[Emim][OAc] mixtures of various ratios, and the endothermic characteristics are summarized in Table 1. The axes scales in the figures are made the same for better comparison of the results of different starches.

[Insert Figure 2 here]

[Insert Table 1 here]

There are several known transitions that can be seen in the DSC results of the different starches. It can be seen from Figure 2a that for WMS in pure water, there was a single well-defined endothermic peak between 64 °C to 84 °C, which is undoubtedly attributed to the gelatinization (G) of amylopectin (Liu, Yu, Xie, & Chen, 2006; Perry, & Donald, 2000, 2002; Tan, Wee, Sopade, & Halley, 2004). An additional peak termed M1, which usually appears at low water or plasticizer content (Liu et al., 2006; Liu et al., 2011), reflecting the helix-coil transformation associated with the unwinding of amylopectin double helices and loss of the starch granular birefringence (Waigh, Gidley, Komanshek, & Donald, 2000), was not observed here. The gelatinization peak, G, related to the transition from smectic to nematic phase for B-type starches such as G50 and G80, and from smectic to isotropic phase for A-type starches such as WMS and RMS (Waigh et al., 2000), appears to have completely overlapped with the M1 transition because of the excess of water/[Emim][OAc] used. The M2 transition is related to the

phase transition of amylose-lipid complex (Biliaderis, Page, Slade, & Sirett, 1985; Jovanovich, & Añón, 1999; Raphaelides, & Karkalas, 1988), and, as expected, was not observed for WMS because of their rather low amylose content, but it was observed for G50 and G80. With the variation in the water/[Emim][OAc] ratio from pure water to 25.0/1 mol/mol, the gelatinization peak moved to a higher temperature accompanied with a greater ΔH (cf. Figure 2a and Table 1).

Microscopic images in Figure 3 substantiate the increase in the gelatinization temperature as, while there was no apparent change in starch granules at the T_o, almost all the granules were destroyed with the absence of the birefringence at the T_c. However, a further decrease in the water/[Emim][OAc] ratio resulted in the gelatinization peak moving towards a lower temperature and the area under the peak becoming smaller. When the ratio was changed to 7.2/1 mol/mol, the gelatinization peak shifted to a lower temperature (between 35 °C and 48 °C) accompanied by an exothermic peak that partially overlapped this peak at lower temperature. The gelatinization peak in this case appeared relatively moderate (i.e., with reduced enthalpy, compared to the other peaks at lower [Emim][OAc] content) with a possible reason being that it has been offset by the exothermic transition. From the microscopic images in Figure 3, it can be seen that immediately after the endothermic and exothermic transitions (i.e. 48 °C), the granules were largely swollen and even destroyed, although some granules were still retained and showed birefringence. The granules were completely destroyed at 100 °C, suggesting that the granules continued to be broken down between 48 °C and 100 °C even though there were no DSC peaks found in this temperature range.

[Insert Figure 3 here]

When the 0.1/1 water–[Emim][OAc] mixture was used, a very large and broad exothermic peak occurred with its peak at a temperature as high as 88 °C. In this case, no endothermic transition like gelatinization was observed. This could be either that an endothermic transition did not occur or that it did, but was concealed by the large exothermic transition. Microscopy (Figure 3) further shows that gelatinization had not started before 48 °C (the T_c in the 7.2/1 water–[Emim][OAc] mixture); however, complete disruption of granular and crystalline structures did occur between 48 °C and 100 °C (or somewhere during the exothermic transition).

It can be seen from Figure 2 and Table 1 that the water/[Emim][OAc] ratio had a very similar effect on the phase transition behavior of RMS, G50, and G80, as it did on that of WMS as reported above. With higher amylose content, the gelatinization peak became less sharp and even appeared as a shoulder, which is believed to be related to the phase transition of amylose-lipid complex (M2) (Biladeris, Page, Slade, & Sirett, 1985; Jovanovich, & Añón, 1999; Raphaelides, & Karkalas, 1988). From the microscopic images in Figure 3, it can be seen that there had already been some degree of change for RMS in the 25.0/1 water–[Emim][OAc] mixture before the T_o. This change, however, was not evident for G50 and G80. The microscopic images also show that the granules, while swollen, were not fully solubilized at the T_c for these starches in pure water or the 25.0/1 water–[Emim][OAc] mixture. G50 and G80 even maintained some intact granules at the T_c. This is no surprise since high amylose starches like G50 and G80 are known to have difficulty in reaching complete gelatinization (Chen, Yu, Kealy, Chen, & Li, 2007; Liu et al., 2006; Liu et al., 2011). Gelatinization of these high amylose materials typically requires higher temperatures or shear treatment.

With the decrease in water/[Emim][OAc] ratio from pure water to 96.0/1 mol/mol, and then to 25.0/1 mol/mol, the ΔH first increased and then decreased for RMS, G50, and G80, which is

different from the case of WMS. This trend was more prominent when the amylose content was higher. In addition to these, it is noteworthy that the exothermic transition for the four starches in the 7.2/1 water–[Emim][OAc] mixture gradually moved to higher temperature (33 °C, 40 °C, 41 °C, and 47 °C, respectively) with higher amylose content. However, when the 0.1/1 water–[Emim][OAc] mixture was used, this trend was not observed. Nonetheless, RMS had a higher peak temperature of the large exothermic transition than any other maize starch. The microscopic results show that while RMS and G50 showed similar results to WMS — in that the 7.2/1 water–[Emim][OAc] mixture displayed some degree of change before the T_c of the endothermic/exothermic transition — much less change was observed for G80. Again, in the 7.2/1 water–[Emim][OAc] mixture, most of the structural change occurred at higher temperature than the T_c. In the 0.1/1 water–[Emim][OAc] mixture, higher temperature was needed for the structural breakdown to start, when compared to the 7.2/1 water–[Emim][OAc] mixture.

3.2. Effect of water/[Emim][OAc] ratio on the pasting properties of maize starches with different amylose contents.

Figure 4 shows the RVA results of maize starches with different amylose contents as affected by the water/[Emim][OAc] ratio; and the characteristic parameters of RVA pasting curves are summarized in Table 2. The axes scales of the figures are made the same for better comparison of the results from different starches.

[Insert Figure 4 here]

[Insert Table 2 here]

It can be seen from Figure 4a that the water/[Emim][OAc] ratio had a significant impact on the RVA profile of WMS. The pasting temperature of WMS in pure water was 72 °C; and this temperature was increased to 81 °C and to 82 °C for the sample in the 96.0/1 water–[Emim][OAc] mixture and the 25.0/1 water–[Emim][OAc] mixture, respectively (cf. Table 2). However, when the water/[Emim][OAc] ratio was further reduced to 7.2/1 mol/mol, the pasting temperature decreased to < 50 °C. This shows the same trend as observed by DSC.

It is no surprise to see the difference between the pasting temperature obtained by RVA and the T_o obtained by DSC as the change in crystalline structures should be prior to the increase in viscosity as a result of granular swelling during gelatinization. Previous studies (Liu, Lelievre, & Ayoung-Chee, 1991; Xie, Yu, Chen, & Li, 2008) have also shown that different techniques detect starch gelatinization in different ways giving slightly different values. On the other hand, the decrease in water/[Emim][OAc] ratio resulted in an upward shift of the entire pasting curve to higher viscosity values. This is especially the case for the sample in the 7.2/1 water–[Emim][OAc] mixture. The peak viscosity is as high as 14235 RVU, which is much higher than those (3741 RVU, 3795 RVU, and 4411 RVU, respectively) of the samples in pure water, in the 96.0/1 water–[Emim][OAc] mixture, and in the 25.0/1 water–[Emim][OAc] mixture.

However, when the 0.1/1 water–[Emim][OAc] mixture was used, a different curve profile was observed. The pasting temperature (80.6 °C) was similar to that of the sample in the 96.0/1 water–[Emim][OAc] mixture and the peak viscosity was lower than those in all other cases. In the 0.1/1 water–[Emim][OAc] mixture, the breakdown viscosity was small but there was a relatively big setback viscosity (cf. Table 2). Furthermore, the final viscosity of WMS in the different mixtures were in the order pure water < 96.0/1 mol/mol < 25.0/1 mol/mol < 7.2/1

mol/mol < 0.1/1 mol/mol (cf. Figure 4), corresponding to, but not necessarily solely contributed by, the viscosity of the mixture.

From Figure 4b–d and Table 2, it can be observed that WMS, RMS, G50, and G80 also showed the same effects of water/[Emim][OAc] ratio on pasting temperature and viscosity. Again, the effects from RVA corresponded well to the results from DSC, except that the gelatinization temperature of the samples in the 0.1/1 water–[Emim][OAc] mixture could not be detected by DSC. It is also worth noting that the final viscosity of RMS in the 7.2/1 water–[Emim][OAc] mixture was lower than in the other mixtures. Another noteworthy fact is that high-amylose starches G50 and G80 showed irregular RVA curves because of their difficulty to gelatinize; i.e., they required much higher temperatures to complete gelatinization (Liu et al., 2006). Trough viscosity could not be easily identified, as an increase in viscosity during temperature holding at 95 °C could be observed in some cases. This could be due to the fact that a prolonged process of granular swelling (which resulted in a viscosity increase) occurred in parallel with the granular disruption (which contributed to a viscosity decrease). This is especially the case for G50 in the 25.0/1 water–[Emim][OAc] mixture. Moreover, negligible or very small increases in viscosity were observed for G80 in pure water, or in the 96.0/1 or 25.0/1 water–[Emim][OAc] mixtures, showing very limited granular swelling. However, in the case of G50 or G80 in the 7.2/1 water–[Emim][OAc] mixture, a prominent increase in viscosity and a typical RVA curve pattern could still be observed, representing the "gelatinization process" and the following pasting behavior, which is in contrast to the results from DSC where no endothermic transition could be found. The initial viscosity increases in this case were much more remarkable that those of G50 and G80 in the 0.1/1 water–[Emim][OAc] mixture. Furthermore, while the final viscosity as a result of a strong setback for WMS, RMS, and G50 in

345 the 0.1/1 water–[Emim][OAc] mixture was higher than those of these samples in the aqueous
346 mixtures, this was not the case for G80, of which the final viscosity in the 0.1/1 water–
347 [Emim][OAc] mixture was much lower than that in the 7.2/1 water–[Emim][OAc] mixture.
348 Figure 5 shows the microscopic images of the four starches before and after the RVA process.
349 Compared with the native starches which have intact granules and bright birefringence patterns,
350 the samples after the RVA process have different degrees of gelatinization as influenced by the
351 water/[Emim][OAc] mixtures.
352
353 [Insert Figure 5 here]
354
355 For WMS, full gelatinization in any of the mixtures could be confirmed by both the normal
356 light images which show complete dissolution except for just a few granular remains and the
357 polarized light images which show no residual polarization (black).
358 For RMS, pure water and the 96.0/1 (not shown in the figure) and 25.0/1 water–[Emim][OAc]
359 mixtures resulted in a textural pattern under normal light, despite that no birefringence was
360 observed under polarized light. This textural pattern, however, was not shown for RMS in the
361 7.2/1 water–[Emim][OAc] mixture. This could correspond to the lower final viscosity of RMS
362 in the 7.2/1 water–[Emim][OAc] mixture as mentioned above. Full dissolution was also
363 observed for RMS in the 0.1/1 water–[Emim][OAc] mixture.
364 For high-amylose starches such as G50 and G80, the granules, though expanded, were
365 largely retained after RVA treatment with pure water, or the 96.0/1 (not shown in the figure) or
366 25.0/1 water–[Emim][OAc] mixture. The polarized light images show very slight birefringence
367 for G80 in the 96.0/1 (not shown in figure) or 25.0/1 water–[Emim][OAc] mixtures. It is known

that, at least in pure water, G50 and G80 cannot be fully gelatinized under 95 °C (the highest temperature used in RVA) (Liu et al., 2006). Nevertheless, the granules became blurred and no birefringence could be observed after RVA treatment with the 7.2/1 water–[Emim][OAc] mixture. Complete dissolution was observed for all the starches in pure [Emim][OAc] after RVA treatment.

4. Discussion

4.1. Gelatinization vs. dissolution (endothermic transition vs. exothermic transition).

Our discussion starts with WMS because it is considered especially interesting due to its high amylopectin component. As shown in the DSC (Figure 2) and RVA (Figure 4) data above, a decrease in water/[Emim][OAc] ratio from pure water to 25.0/1 mol/mol resulted in an increase in the gelatinization temperatures, but a further decrease to 7.2/1 water/[Emim][OAc] molar ratio contributed to a decrease in the gelatinization temperature. Though DSC could not reveal the gelatinization process (only a large exothermic peak was observed) in the 2.8/1 or 0.1/1 water–[Emim][OAc] mixture, microscopic images (cf. Figure 3) and RVA results (cf. Figure 4) showed that "gelatinization" was moved to a higher temperature (a temperature similar to that of the sample in the 96.0/1 water–[Emim][OAc] mixture). Similarly, Liu, & Budtova (2012) also observed an unexpected effect of water/[Emim][OAc] on the phase transition of WMS.

The unexpected trend described above lead us to consider that two processes control the phase transition of starch in the water–[Emim][OAc] mixtures, i.e., gelatinization and dissolution. Gelatinization is known to be an endothermic process which requires energy to break the internal hydrogen bonds and to melt the native crystalline structures. In gelatinization, granular swelling and disruption occur before molecular solubilization. It has been shown by nuclear magnetic

391 resonance (NMR) spectroscopy and molecular dynamics that solvation involves the formation of
392 hydrogen bonds between the anions of the imidazolium salt and the hydroxyl hydrogen atoms of
393 the carbohydrate in approximately a stoichiometric ratio (Moulthrop, Swatloski, Moyna, &
394 Rogers, 2005; Novoselov, Sashina, Petrenko, & Zaborsky, 2007; Remsing, Swatloski, Rogers, &
395 Moyna, 2006; Youngs et al., 2006; Youngs, Hardacre, & Holbrey, 2007). The dissolution of
396 starch in [Emim][OAc] appears to be an exothermic process possibly due to the interaction
397 between starch and [Emim][OAc].
398 Koganti, Mitchell, Ibbett, & Foster (2011) studied the thermal transitions of starch in a
399 mixture of water and *N*-methyl morpholine *N*-oxide (NMMO) (starch concentration in the mixed
400 liquid was fixed at 10%) and found that, while there was an endothermic transition when the
401 water/NMMO ratio was high, an exothermic transition appeared when NMMO became the major
402 component in the mixture liquid. Liu et al. (2011) suggested that the –OH bond interaction
403 between dried starch and glycerol could generate a great amount of heat during "solvation of
404 plasticizer" with increasing temperature. Therefore in this study, the type of transition
405 (endothermic or exothermic) could demonstrate whether complete gelatinization or direct
406 dissolution played a major role.
407 In the case of WMS in pure water or the 96.0/1, or 25.0/1 water–[Emim][OAc] mixture,
408 dissolution was negligible or only played a minor role before and/or simultaneously with the
409 gelatinization process in the phase transition. This can be demonstrated by the microscopic
410 images in Figure 3 which show little change in starch until the T_o of gelatinization. For RMS,
411 G50, and G80, the dissolution could play some role before and/or along with the gelatinization
412 process when the water/[Emim][OAc] molar ratio was 25.0/1, as shown by a decrease in the ΔH,
413 and the microscopic results (especially of RMS).

At a water/[Emim][OAc] molar ratio of 7.2/1, the dissolution played the dominant role as evidenced by the exothermic peak and the reduced (for WMS and RMS) or absent (for G50 and G80) gelatinization peak. For WMS and RMS, the dissolution process in 7.2/1 water–[Emim][OAc] mixture could "disrupt" the native granular structure, facilitating partial crystalline melting (cf. Figure 2) and granular swelling at lower temperature. Granular swelling would involve the trapping of water and/or [Emim][OAc] molecules into amylopectin aggregates, resulting in a viscosity increase as shown in Figure 4. Further gradual dissolution disrupts the remaining granular and crystalline structures. Also dissolution enabled G50 and G80 to undergo granular swelling at higher temperature, as evidenced by an increase in viscosity measured by RVA (cf. Figure 4). Despite the granular swelling, it is considered that the crystalline structure of G50 and G80 was completely destroyed by dissolution rather than traditional melting since no endothermic transition was observed in the DSC (cf. Figure 2 and Figure 3).

For all the starches, the 7.2/1 water–[Emim][OAc] mixture contributed to a higher degree of structural disruption and dissolution at the end of the RVA test than any other mixture with higher water/[Emim][OAc] ratios (cf. Figure 4). This conclusion was not confirmed by the final viscosity, however other factors such as the amylose/amylopectin ratio in starch, the degree of gelatinization/dissolution, the molecular weight of the starch molecules dissolved, and the related sensitivity to shear treatment and solubility (accounting for the viscosity breakdown) and retrogradation (accounting for the viscosity setback) could be in play here. Another thing that is worth noting here is that the exothermic peak moved to higher temperature with an increase in amylose content (cf. Figure 2). This might demonstrate that the higher the amylose content, the more difficult is it for the dissolution to take place because of the more compact structure (Chen et al., 2009).

For all the starches in the 0.1/1 water–[Emim][OAc] mixture compared to those in 7.2/1 water–[Emim][OAc] mixtures, the phase transition occurred at higher temperature (as seen in microscopic images in Figure 3 and RVA results in Figure 4). While it is difficult to know if an endothermic transition representing the crystalline melting occurred because of the large exothermic peak covering a wide temperature range, it could be proposed that the lack of water resulted in the delay of the phase transition. Specifically, the absence of water in the solution allowed more free hydroxyl groups in starch to interact with [Emim][OAc] (demonstrated by the large exothermic peak) whilst in other mixtures water interacted with some hydroxyl groups in starch, leaving less for the interaction with [Emim][OAc].

Accompanied by the gradual starch–[Emim][OAc] interaction, a moderate increase in viscosity with very small viscosity breakdown in RVA (cf. Figure 4) demonstrated that the granular swelling and the structural disruption and dissolution happened simultaneously and continuously during temperature increasing to and holding at 95 °C. Furthermore, a higher degree of dissolution of starch molecules could be favorable for retrogradation during cooling, resulting in a large viscosity setback in the 0.1/1 water–[Emim][OAc] mixture (cf. Figure 4).

4.2. Role of the ionic liquid (gelatinization agent vs. solvent).

The concentration of [Emim][OAc] in the solution and the related solution viscosity could play important roles in the dissolution of starch. The basicity of IL anions is primarily responsible for the dissolution of biopolymers (Remsing et al., 2006). When starch granules are dispersed in [Emim][OAc], the IL is able to sequentially destroy the semicrystalline structure of native starch granules and disrupt the intermolecular and intramolecular hydrogen bonding network between hydroxyl groups of starch biopolymer.

Water acts as an anti-solvent and the strong interactions between water and the IL ions are also exothermic. Water can effectively tie up acetate ions forming acetic acid and strong hydrogen bonds which prevent acetate–starch hydrogen bonding. When large amounts of water are present (water/[Emim][OAc] ≥ 25.0/1 mol/mol), there is not enough $[OAc]^-$ to interact with the polymer and gelatinization will be the dominant process over dissolution. When larger amounts of [Emim][OAc] are present (water/[Emim][OAc] ≤ 10.8/1 mol/mol), more "free" acetate anions are available to disrupt the starch hydrogen bonding network and solubilize the starch.

When the water/[Emim][OAc] ratios are 10.8/1 mol/mol or 7.2/1 mol/mol, there can be both some free $[OAc]^-$ anions to interact with starch for a dissolution function, and some free water to interact with starch, for a gelatinization function. Here gelatinization and dissolution occurs simultaneously, as water and [Emim][OAc] are both interacting with starch hydroxyls (possibly in a competitive way).

When [Emim][OAc] at high concentration (water/[Emim][OAc] ≥ 2.8/1 mol/mol) is used, the interaction between $[OAc]^-$ anions and starch hydroxyl groups might be restricted by insufficient penetration through crystalline regions at lower temperatures. Nevertheless, the exact cause will be probed in future work.

5. Conclusions

This study suggests that gelatinization and/or dissolution account(s) for the phase transition of various starch systems and the water/[Emim][OAc] ratio determines whether gelatinization or dissolution plays the dominant role. In contrast to gelatinization which is known to be an endothermic process, dissolution involves the interaction between starch hydroxyl groups and

483 $[OAc]^-$ anions, which is an exothermic process. At high water/[Emim][OAc] ratios (> 25.0/1
484 mol/mol), the strong interactions between [Emim][OAc] and water decrease the available free
485 [Emim][OAc] making dissolution more difficult, and thus gelatinization is mainly responsible
486 for the phase transition of the starch. The < 7.2/1 water–[Emim][OAc] mixture represents a
487 solvent for which the phase transition of starch is predominantly influenced by dissolution.
488 Dissolution by [Emim][OAc] can have the same impact as, and/or assist, gelatinization by water
489 in disruption of starch native granular and crystalline structures. In this case, water and
490 [Emim][OAc] competitively interact with starch but play a synergistic role in the phase transition.
491 The dissolution process, however, become less easy when water is absent in the system, which
492 may be due to decreased diffusion to or through the starch. While starch with higher amylose
493 content is generally more difficult to be dissolved/gelatinized, the effect of water/[Emim][OAc]
494 ratio on the gelatinization/dissolution of different starches shows similar patterns.
495 While pure IL is widely used to dissolve polysaccharides, this study demonstrates that there
496 is a water–[Emim][OAc] mixture of specific ratio (7.2/1 mol/mol) that is effective in disruption
497 of starch native granular and crystalline structures at reduced temperature. In addition, different
498 types of starch products (e.g. soluble starch, pre-gelatinized starch, starch solutions of different
499 viscosities, etc.) could be generated by using starches with different amylose contents and water–
500 [Emim][OAc] mixtures of different ratios. Further understanding of the mechanism of
501 gelatinization/dissolution of starch in water–[Emim][OAc] mixtures would allow the design of
502 solvents for a wide range of starch applications such as production of plasticized starch and
503 chemical modification of starch. Work is currently under way in our laboratories toward this end.
504

Acknowledgements

The research leading to these results has received funding from the Australian Research Council (ARC) under the Discovery Project 120100344. S. Mateyawa, also would like to thank the iTaukei Affairs Scholarship Scheme (IASS) by the Ministry of iTaukei Affairs, Fiji for providing research funding for her PhD studies at The University of Queensland (UQ). Acknowledgements are also made to Dr. Jovin Hasjim, Centre for Nutrition & Food Sciences, Queensland Alliance for Agriculture and Food Innovation, UQ for his kind discussion with the authors on the mechanism in this study, to Dr. Gleb E. Yakubov, School of Chemical Engineering, UQ, for the proofreading of the manuscript, and to A/Prof. Jason R. Stokes, School of Chemical Engineering, UQ, for providing the rheometer used in this study.

References

Atwell, W. A., Hood, L. F., Lineback, D. R., Varrianomarston, E., & Zobel, H. F. (1988). The terminology and methodology associated with basic starch phenomena. *Cereal Foods World, 33*(3), 306-311.

Biladeris, C. G., Page, C. M., Slade, L., & Sirett, R. R. (1985). Thermal behavior of amylose-lipid complexes. *Carbohydrate Polymers, 5*, 367-389.

Biliaderis, C. G., Page, C. M., Slade, L., & Sirett, R. R. (1985). Thermal behavior of amylose-lipid complexes. *Carbohydrate Polymers, 5*(5), 367-389.

Biswas, A., Shogren, R. L., Stevenson, D. G., Willett, J. L., & Bhowmik, P. K. (2006). Ionic liquids as solvents for biopolymers: Acylation of starch and zein protein. *Carbohydrate Polymers, 66*(4), 546-550.

Chaudhary, A. L., Miler, M., Torley, P. J., Sopade, P. A., & Halley, P. J. (2008). Amylose content and chemical modification effects on the extrusion of thermoplastic starch from maize. *Carbohydrate Polymers, 74*(4), 907-913.

Chaudhary, A. L., Torley, P. J., Halley, P. J., McCaffery, N., & Chaudhary, D. S. (2009). Amylose content and chemical modification effects on thermoplastic starch from maize - Processing and characterisation using conventional polymer equipment. *Carbohydrate Polymers, 78*(4), 917-925.

Chen, P., Yu, L., Kealy, T., Chen, L., & Li, L. (2007). Phase transition of starch granules observed by microscope under shearless and shear conditions. *Carbohydrate Polymers, 68*(3), 495-501.

Chen, P., Yu, L., Simon, G., Petinakis, E., Dean, K., & Chen, L. (2009). Morphologies and microstructures of cornstarches with different amylose-amylopectin ratios studied by confocal laser scanning microscope. *Journal of Cereal Science, 50*(2), 241-247.

Davies, G. A., & Stokes, J. R. (2005). On the gap error in parallel plate rheometry that arises from the presence of air when zeroing the gap. *Journal of Rheology, 49*(4), 919-922.

Davies, G. A., & Stokes, J. R. (2008). Thin film and high shear rheology of multiphase complex fluids. *Journal of Non-Newtonian Fluid Mechanics, 148*(1-3), 73-87.

El Seoud, O. A., Koschella, A., Fidale, L. C., Dorn, S., & Heinze, T. (2007). Applications of Ionic Liquids in Carbohydrate Chemistry: A Window of Opportunities. *Biomacromolecules, 8*(9), 2629-2647.

Jovanovich, G., & Añón, M. C. (1999). Amylose–lipid complex dissociation. A study of the kinetic parameters. *Biopolymers, 49*(1), 81-89.

549 Kärkkäinen, J., Lappalainen, K., Joensuu, P., & Lajunen, M. (2011). HPLC-ELSD analysis of six
550 starch species heat-dispersed in [BMIM]Cl ionic liquid. *Carbohydrate Polymers, 84*(1), 509-
551 516.
552 Koganti, N., Mitchell, J. R., Ibbett, R. N., & Foster, T. J. (2011). Solvent Effects on Starch
553 Dissolution and Gelatinization. *Biomacromolecules, 12*(8), 2888-2893.
554 Lelievre, J. (1974). Starch gelatinization. *Journal of Applied Polymer Science, 18*(1), 293-296.
555 Leroy, E., Jacquet, P., Coativy, G., Reguerre, A. l., & Lourdin, D. (2012). Compatibilization of
556 starch–zein melt processed blends by an ionic liquid used as plasticizer. *Carbohydrate*
557 *Polymers, 89*(3), 955-963.
558 Li, M., Liu, P., Zou, W., Yu, L., Xie, F., Pu, H., Liu, H., & Chen, L. (2011). Extrusion
559 processing and characterization of edible starch films with different amylose contents.
560 *Journal of Food Engineering, 106*(1), 95-101.
561 Liew, C.-W., Ramesh, S., Ramesh, K., & Arof, A. (2012). Preparation and characterization of
562 lithium ion conducting ionic liquid-based biodegradable corn starch polymer electrolytes.
563 *Journal of Solid State Electrochemistry, 16*(5), 1869-1875.
564 Liu, H., Lelievre, J., & Ayoung-Chee, W. (1991). A study of starch gelatinization using
565 differential scanning calorimetry, X-ray, and birefringence measurements. *Carbohydrate*
566 *Research, 210*, 79-87.
567 Liu, H., Yu, L., Xie, F., & Chen, L. (2006). Gelatinization of cornstarch with different
568 amylose/amylopectin content. *Carbohydrate Polymers, 65*(3), 357-363.
569 Liu, H., Xie, F., Yu, L., Chen, L., & Li, L. (2009). Thermal processing of starch-based polymers.
570 *Progress in Polymer Science, 34*(12), 1348-1368.

Liu, P., Xie, F., Li, M., Liu, X., Yu, L., Halley, P. J., & Chen, L. (2011). Phase transitions of maize starches with different amylose contents in glycerol-water systems. *Carbohydrate Polymers, 85*(1), 180-187.

Liu, W., & Budtova, T. (2012). Dissolution of unmodified waxy starch in ionic liquid and solution rheological properties. *Carbohydrate Polymers, x*(x), In press. dx.doi.org/10.1016/j.carbpol.2012.1001.1090.

Moulthrop, J. S., Swatloski, R. P., Moyna, G., & Rogers, R. D. (2005). High-resolution 13C NMR studies of cellulose and cellulose oligomers in ionic liquid solutions. *Chemical Communications*(12), 1557-1559.

Novoselov, N., Sashina, E., Petrenko, V., & Zaborsky, M. (2007). Study of dissolution of cellulose in ionic liquids by computer modeling. *Fibre Chemistry, 39*(2), 153-158.

Pérez, S., & Bertoft, E. (2010). The molecular structures of starch components and their contribution to the architecture of starch granules: a comprehensive review. *Starch/Stärke, 62*(8), 389-420.

Perry, P. A., & Donald, A. M. (2000). The Role of Plasticization in Starch Granule Assembly. *Biomacromolecules, 1*(3), 424-432.

Perry, P. A., & Donald, A. M. (2002). The effect of sugars on the gelatinisation of starch. *Carbohydrate Polymers, 49*(2), 155-165.

Ramesh, S., Liew, C.-W., & Arof, A. K. (2011). Ion conducting corn starch biopolymer electrolytes doped with ionic liquid 1-butyl-3-methylimidazolium hexafluorophosphate. *Journal of Non-Crystalline Solids, 357*(21), 3654-3660.

Ramesh, S., Shanti, R., Morris, E., & Durairaj, R. (2011). Utilisation of corn starch in production of 'green' polymer electrolytes. *Materials Research Innovations, 15*(1), s8.

Ramesh, S., Shanti, R., & Morris, E. (2012). Studies on the thermal behavior of CS:LiTFSI:[Amim] Cl polymer electrolytes exerted by different [Amim] Cl content. *Solid State Sciences, 14*(1), 182-186.

Raphaelides, S., & Karkalas, J. (1988). Thermal dissociation of amylose-fatty acid complexes. *Carbohydrate Research, 172*(1), 65-82.

Ratnayake, W. S., Jackson, D. S., & Steve, L. T. (2008). Starch gelatinization. *Advances in Food and Nutrition Research, 55*, 221-268.

Remsing, R. C., Swatloski, R. P., Rogers, R. D., & Moyna, G. (2006). Mechanism of cellulose dissolution in the ionic liquid 1-n-butyl-3-methylimidazolium chloride: a 13C and 35/37Cl NMR relaxation study on model systems. *Chemical Communications*(12), 1271-1273.

Russo, M. A. L., O'Sullivan, C., Rounsefell, B., Halley, P. J., Truss, R., & Clarke, W. P. (2009). The anaerobic degradability of thermoplastic starch: polyvinyl alcohol blends: potential biodegradable food packaging materials. *Bioresource Technology, 100*(5), 1705-1710.

Sankri, A., Arhaliass, A., Dez, I., Gaumont, A. C., Grohens, Y., Lourdin, D., Pillin, I., Rolland-Sabaté, A., & Leroy, E. (2010). Thermoplastic starch plasticized by an ionic liquid. *Carbohydrate Polymers, 82*(2), 256-263.

Stevenson, D. G., Biswas, A., Jane, J.-l., & Inglett, G. E. (2007). Changes in structure and properties of starch of four botanical sources dispersed in the ionic liquid, 1-butyl-3-methylimidazolium chloride. *Carbohydrate Polymers, 67*(1), 21-31.

Tan, I., Wee, C. C., Sopade, P. A., & Halley, P. J. (2004). Investigation of the starch gelatinisation phenomena in water-glycerol systems: application of modulated temperature differential scanning calorimetry. *Carbohydrate Polymers, 58*(2), 191-204.

616 Tan, I., Flanagan, B. M., Halley, P. J., Whittaker, A. K., & Gidley, M. J. (2007). A method for
617 estimating the nature and relative proportions of amorphous, single, and double-helical
618 components in starch granules by ^{13}C CP/MAS NMR. *Biomacromolecules, 8*(3), 885-891.
619 Torley, P. J., Rutgers, R. P. G., D'Arcy, B., & Bhandari, B. R. (2004). Effect of honey types and
620 concentration on starch gelatinization. *LWT--Food Science and Technology, 37*(2), 161-170.
621 Waigh, T. A., Gidley, M. J., Komanshek, B. U., & Donald, A. M. (2000). The phase
622 transformations in starch during gelatinisation: a liquid crystalline approach. *Carbohydrate*
623 *Research, 328*(2), 165-176.
624 Wang, J., Yu, L., Xie, F., Chen, L., Li, X., & Liu, H. (2010a). Rheological properties and phase
625 transition of cornstarches with different amylose/amylopectin ratios under shear stress.
626 *Starch/Stärke, 62*(12), 667-675.
627 Wang, N., Zhang, X., Liu, H., & He, B. (2009). 1-Allyl-3-methylimidazolium chloride
628 plasticized-corn starch as solid biopolymer electrolytes. *Carbohydrate Polymers, 76*(3), 482-
629 484.
630 Wang, N., Zhang, X., Wang, X., & Liu, H. (2009). Communications: Ionic liquids modified
631 montmorillonite/thermoplastic starch nanocomposites as ionic conducting biopolymer.
632 *Macromolecular Research, 17*(5), 285-288.
633 Wang, N., Zhang, X., Liu, H., & Han, N. (2010b). Ionically Conducting Polymers Based on
634 Ionic Liquid-Plasticized Starch Containing Lithium Chloride. *Polymers & Polymer*
635 *Composites, 18*(1), 53-58.
636 Wilpiszewska, K., & Spychaj, T. (2011). Ionic liquids: Media for starch dissolution,
637 plasticization and modification. *Carbohydrate Polymers, 86*(2), 424-428.

638 Xie, F., Yu, L., Chen, L., & Li, L. (2008). A new study of starch gelatinization under shear stress
639 using dynamic mechanical analysis. *Carbohydrate Polymers, 72*(2), 229-234.
640 Xie, F., Yu, L., Su, B., Liu, P., Wang, J., Liu, H., & Chen, L. (2009). Rheological properties of
641 starches with different amylose/amylopectin ratios. *Journal of Cereal Science, 49*(3), 371-
642 377.
643 Xie, F., Halley, P. J., & Avérous, L. (2012). Rheology to understand and optimize processibility,
644 structures and properties of starch polymeric materials. *Progress in Polymer Science, 37*(4),
645 595-623.
646 Youngs, T. G. A., Holbrey, J. D., Deetlefs, M., Nieuwenhuyzen, M., Costa Gomes, M. F., &
647 Hardacre, C. (2006). A Molecular Dynamics Study of Glucose Solvation in the Ionic Liquid
648 1,3-Dimethylimidazolium Chloride. *ChemPhysChem, 7*(11), 2279-2281.
649 Youngs, T. G. A., Hardacre, C., & Holbrey, J. D. (2007). Glucose Solvation by the Ionic Liquid
650 1,3-Dimethylimidazolium Chloride: A Simulation Study. *The Journal of Physical Chemistry*
651 *B, 111*(49), 13765-13774.
652 Zakrzewska, M. E., Bogel-Łukasik, E., & Bogel-Łukasik, R. (2010). Solubility of Carbohydrates
653 in Ionic Liquids. *Energy & Fuels, 24*(2), 737-745.
654 Zhu, S., Wu, Y., Chen, Q., Yu, Z., Wang, C., Jin, S., Ding, Y., & Wu, G. (2006). Dissolution of
655 cellulose with ionic liquids and its application: a mini-review. *Green Chemistry, 8*(4), 325-
656 327.
657
658

Figure Captions

Figure 1 Chemical structure of 1-ethyl-3-methylimidazolium acetate ([Emim][OAc]).

Figure 2 DSC results of different starches (a–d: WMS, RMS, G50, and G80, respectively) in water–[Emim][OAc] mixtures of different ratios.

Figure 3 Normal and polarized light (NL and PL, respectively) microscopic images of different native starches, and the related post-DSC samples in water–[Emim][OAc] mixtures of different ratios (pure water, 25.0/1 mol/mol, 7.2/1 mol/mol, and 0.1/1 mol/mol). Refer to Appendix B for the definitions and values of T_1 and T_2.

Figure 4 RVA results of different starches (a–d: WMS, RMS, G50, and G80, respectively) in water–[Emim][OAc] mixtures of different ratios (pure water, 96.0/1 mol/mol, 25.0/1 mol/mol, 7.2/1 mol/mol, and 0.1/1 mol/mol).

Figure 5 Normal and polarized light (NL and PL, respectively) microscopic images of different native starches, and the related post-RVA samples in water–[Emim][OAc] mixtures of different ratios (pure water, 25.0/1 mol/mol, 7.2/1 mol/mol, and 0.1/1 mol/mol).

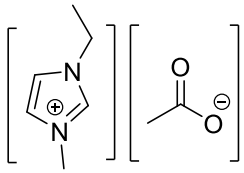

Figure 1

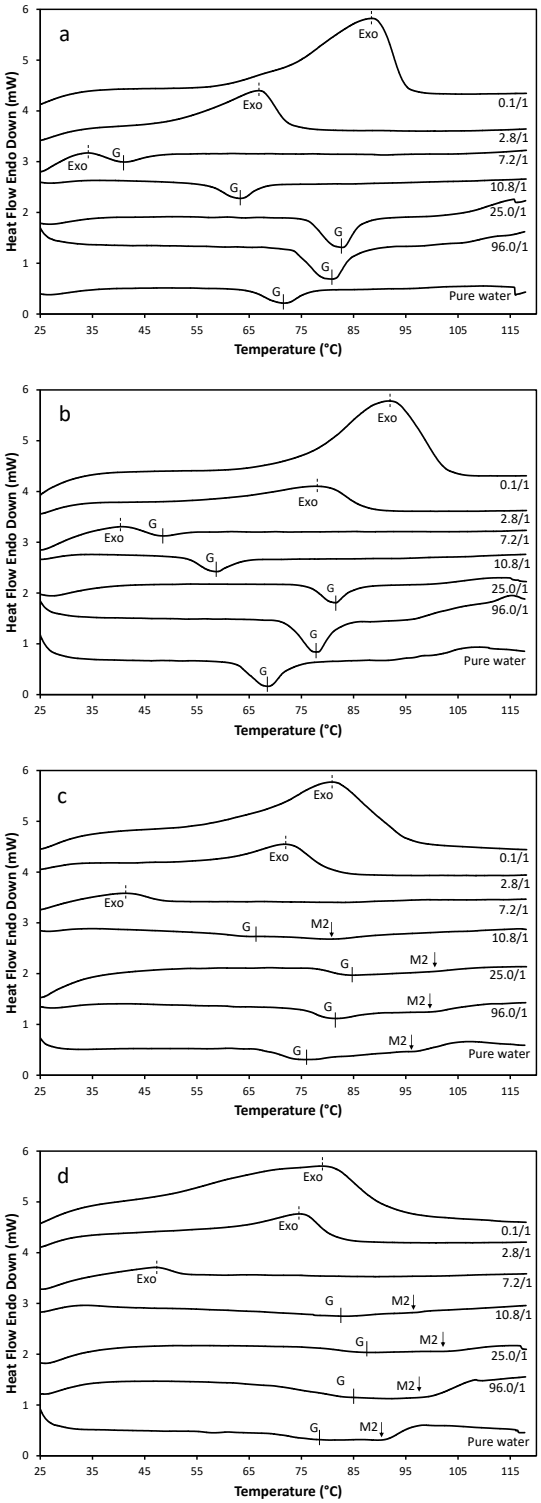
a
b
c
d
Heat Flow Endo Down (mW)
Temperature (°C)
Exo
G
M2
0.1/1
2.8/1
7.2/1
10.8/1
25.0/1
96.0/1
Pure water

Figure 2

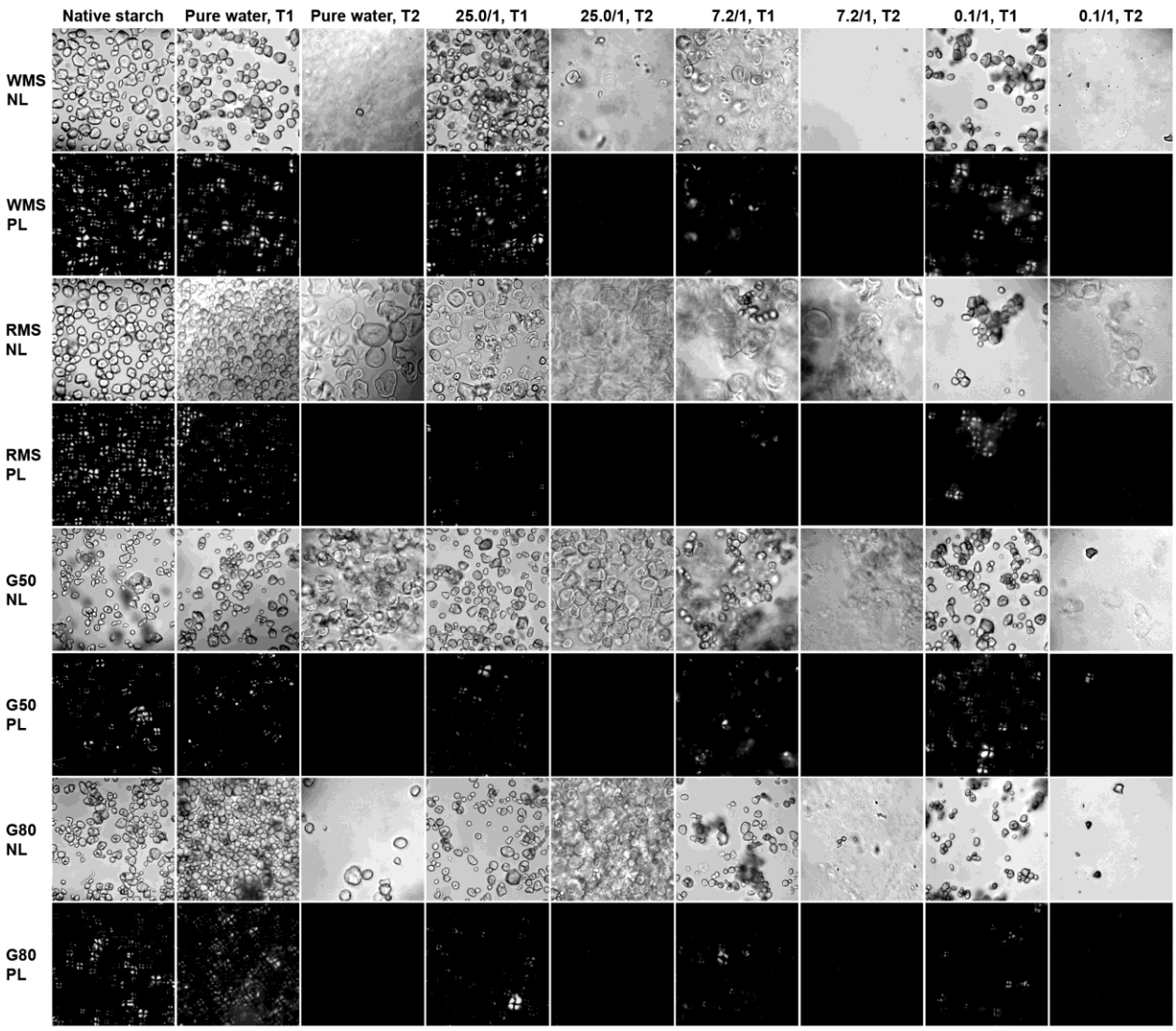
Native starch
Pure water, T1
Pure water, T2
25.0/1, T1
25.0/1, T2
7.2/1, T1
7.2/1, T2
0.1/1, T1
0.1/1, T2
WMS NL
WMS PL
RMS NL
RMS PL
G50 NL
G50 PL
G80 NL
G80 PL

Figure 3

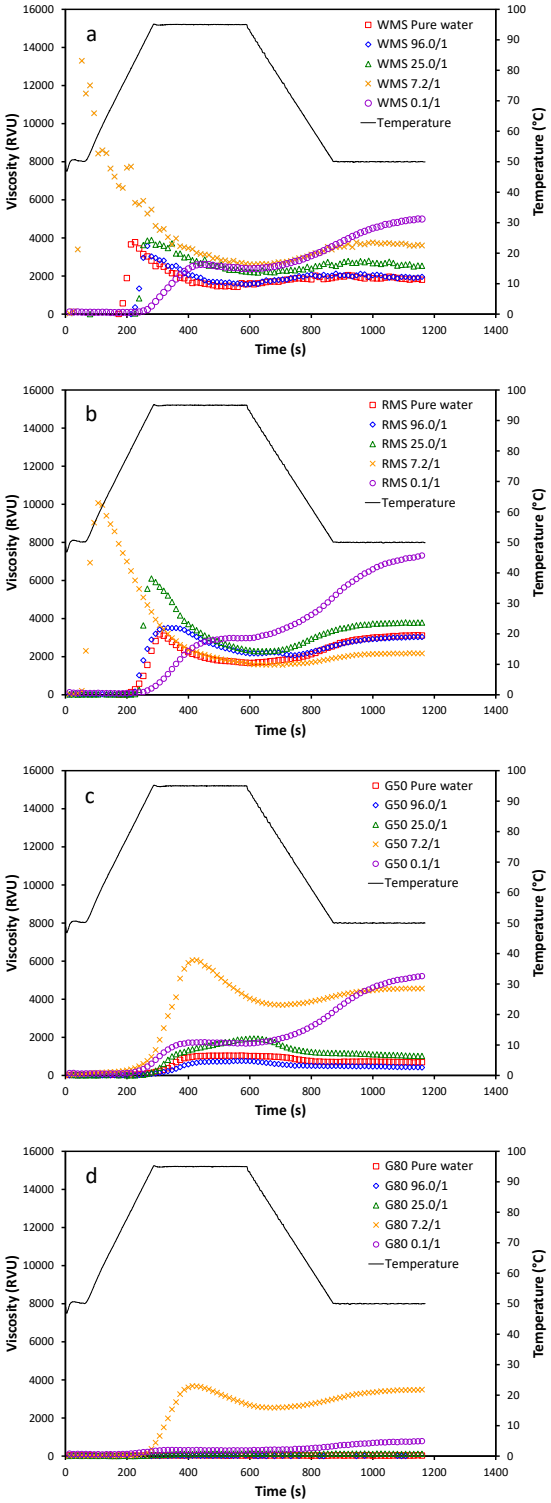
a
WMS Pure water
WMS 96.0/1
WMS 25.0/1
WMS 7.2/1
WMS 0.1/1
Temperature
b
RMS Pure water
RMS 96.0/1
RMS 25.0/1
RMS 7.2/1
RMS 0.1/1
Temperature
c
G50 Pure water
G50 96.0/1
G50 25.0/1
G50 7.2/1
G50 0.1/1
Temperature
d
G80 Pure water
G80 96.0/1
G80 25.0/1
G80 7.2/1
G80 0.1/1
Temperature
Viscosity (RVU)
Temperature (°C)
Time (s)

Figure 4

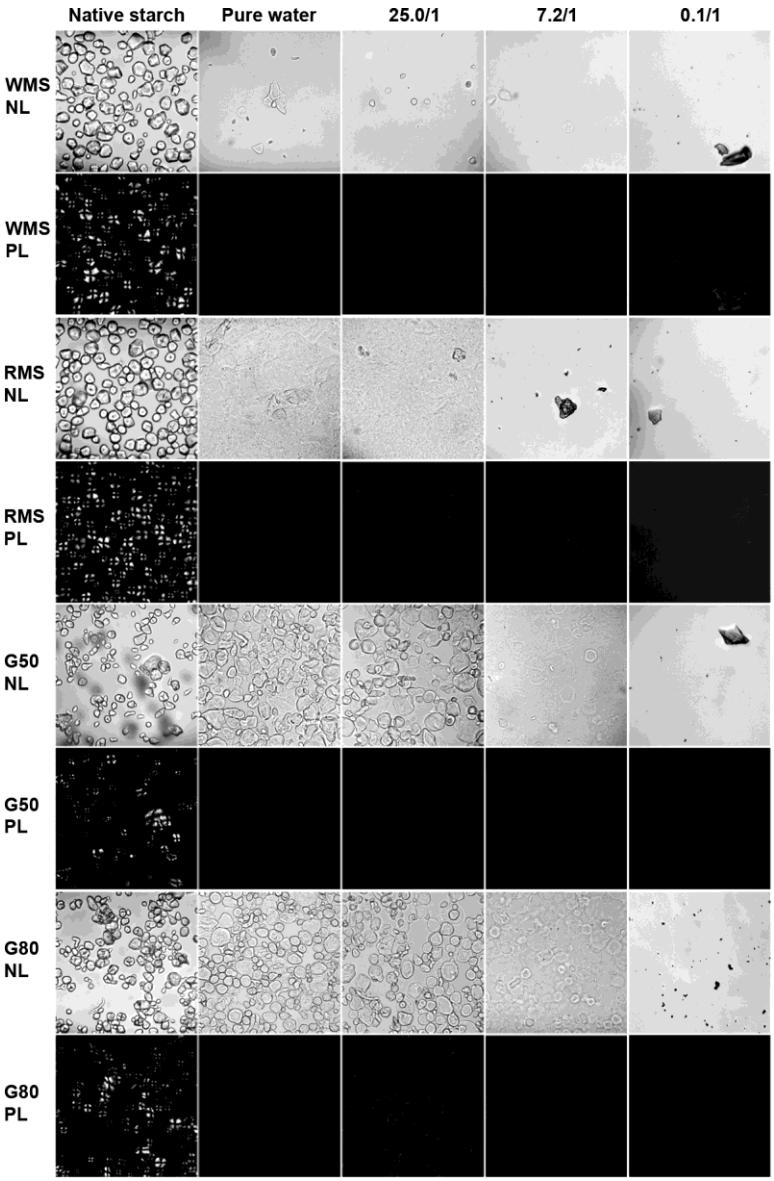
Native starch
Pure water
25.0/1
7.2/1
0.1/1
WMS NL
WMS PL
RMS NL
RMS PL
G50 NL
G50 PL
G80 NL
G80 PL

Figure 5

Tables

Table 1 DSC results of different starches with various water/[Emim][OAc] ratios.

Sample	Water/[Emim][OAc] molar ratio	T_o (°C)	T_p (°C)	T_c (°C)	ΔT (°C)	ΔH (J/g)
WMS	Pure water	64.49±0.09[a]	71.92±0.03	83.80±0.08	19.29±0.00	19.85±0.69
	96.0/1	73.53±0.16	79.82±0.58	91.13±0.00	17.60±0.16	22.17±0.74
	25.0/1	75.78±0.09	82.50±0.56	94.69±0.00	18.91±0.09	27.85±0.60
	10.8/1	57.29±0.12	63.18±0.02	71.67±0.09	14.38±0.03	16.23±0.21
	7.2/1	35.54±0.38	40.83±0.24	47.69±0.05	12.15±0.36	6.95±1.72
	2.8/1	Exothermic peak				
	0.1/1	Exothermic peak				
RMS	Pure water	61.99±0.08	68.27±0.24	80.09±0.07	18.10±0.07	17.60±1.01
	96.0/1	72.36±0.11	77.46±0.26	90.01±0.00	17.66±0.11	17.96±0.30
	25.0/1	76.40±0.40	81.33±0.25	89.21±0.06	12.81±0.40	16.82±1.59
	10.8/1	53.21±0.23	58.70±0.26	67.60±0.07	14.39±0.30	15.88±0.84
	7.2/1	42.47±0.11	47.29±0.14	54.72±0.93	12.25±0.95	6.44±0.30

	2.8/1	Exothermic peak				
	0.1/1	Exothermic peak				
G50	Pure water	67.45±0.08	76.78±0.82	111.21±0.10	43.76±0.17	25.20±1.67
	96.0/1	73.89±1.26	82.10±0.25	112.44±0.09	38.55±1.17	33.56±0.33
	25.0/1	77.91±0.03	85.06±0.04	110.85±0.00	32.94±0.03	24.94±0.70
	10.8/1	54.31±0.09	79.07±0.24	96.01±0.09	41.70±0.18	25.09±1.17
	7.2/1	Exothermic peak				
	2.8/1	Exothermic peak				
	0.1/1	Exothermic peak				
G80	Pure water	66.18±0.79	79.51±0.17	108.27±0.00	42.07±0.75	24.32±1.32
	96.0/1	69.66±1.65	92.48±0.71	108.36±0.08	38.71±1.56	53.08±1.19
	25.0/1	75.70±0.28	88.69±0.65	114.26±0.00	38.57±0.28	32.36±0.06
	10.8/1	Endothermic peak, but too weak to determine				
	7.2/1	Exothermic peak				
	2.8/1	Exothermic peak				
	0.1/1	Exothermic peak				

[a] Standard deviation

Table 2 Characteristic parameters of RVA pasting curves of different starches with various water/[Emim][OAc] ratios.

Sample	Water/[Emim][OAc] molar ratio	Pasting temperature (°C)	Peak viscosity (RVU)	Trough viscosity (RVU)	Final viscosity (RVU)	Breakdown viscosity (RVU)	Setback viscosity (RVU)
WMS	Pure water	72.1	3741	1398	1814	2343	416
	96.0/1	80.7	3795	1609	1901	2186	292
	25.0/1	82.4	4411	2100	2559	2311	459
	7.2/1	<50	14235	2613	3585	11622	972
	0.1/1	80.6	2611	2385	5019	226	2634
RMS	Pure water	74.0	3293	1668	3018	1625	1350
	96.0/1	80.2	3520	2068	3024	1452	956
	25.0/1	84.0	6025	2289	3790	3736	1501
	7.2/1	≤50	10046	1511	2165	8535	654
	0.1/1	79.8	2973	2946	7392	27	4446
G50	Pure water	73.5	1046	–	685	–	–
	96.0/1	81.3	767	–	422	–	–

	25.0/1	86.6	1933	–	1010	–	–
	7.2/1	≤50	6046	3698	4567	2348	869
	0.1/1	75.6	1742	1672	5208	70	3536
G80	Pure water	–	–	–	–	–	–
	96.0/1	–	–	–	–	–	–
	25.0/1	85.8	136	119	136	17	17
	7.2/1	81.2	3180	2542	3482	638	940
	0.1/1	73.8	323	285	781	38	496

Appendices

Appendix A pH values and viscosities of the water–[Emim][OAc] mixtures of different ratios.

Water/[Emim][OAc]/starch mass ratio	Water/[Emim][OAc]/–OH of starch molar ratio[a]	pH (without starch)	pH (with starch)	Viscosity (Pa·s)
10 / 0 / 1	106.50 / 0 / 3.03	7.81	5.34	0.0009±0.0000[b]
9 / 1 / 1	95.99 / 1 / 3.03	6.33	6.31	0.0013±0.0000
7 / 3 / 1	24.99 / 1 / 1.01	6.54	6.50	0.0025±0.0000
5 / 5 / 1	10.79 / 1 / 0.61	7.93	7.79	0.0061±0.0000
4 / 6 / 1	7.24 / 1 / 0.50	8.58	n/a[c]	0.0104±0.0002
2 / 8 / 1	2.81 / 1 / 0.38	10.77	10.58	0.0241±0.0005
0 / 10 / 1	0.14 / 1 / 0.30	13.45	13.73	0.1120±0.0096

[a] The moisture content of starch is taken as 13.6% (average) and 90% purity of [Emim]/[OAc] is considered for calculation.

[b] Standard deviation. [c] Not available for determination due to the solidification.

Appendix B Temperatures used for microscopic observation shown in Figure 3.

Sample	Water/[Emim][OAc] molar ratio	T_1 (°C)[a]	T_2 (°C)[a]
WMS	Pure water	64	84
	25.0/1	75	95
	7.2/1	48	100
	0.1/1	48	100
RMS	Pure water	61	81
	25.0/1	76	90
	7.2/1	55	107
	0.1/1	55	107
G50	Pure water	67	112
	25.0/1	77	111
	7.2/1	50	115
	0.1/1	50	115
G80	Pure water	66	109
	25.0/1	75	115
	7.2/1	55	115
	0.1/1	55	115

[a] For all the starches in pure water or the 22.5/1 water–[Emim][OAc] mixture, $T_1 = T_o$ (DSC) and $T_2 = T_c$ (DSC); for all the starches in the 7.2/1 or 0.1/1 water–[Emim][OAc] mixture, T_1 is the T_c of the endothermic/exothermic transition in 7.2/1 water–[Emim][OAc] mixture and T_2 is the T_c of the exothermic transition in the 0.1/1 water–[Emim][OAc] mixture.